PAPER

Check for updates

Quaternary ammonium eutectogels as a printable, antimicrobial material platform†

Alma Nicolau, [a] Zeyu Shao, [b] Alex C. Bissember, [a] Edgar H. H. Wong, [b] Alexandra L. Mutch *[a] and Stuart C. Thickett *[a]

The solvent-free photopolymerization of a eutectic mixture consisting of a quaternary ammonium methacrylate salt, urea, and functional co-monomer to yield polymeric eutectogels with unique properties and function is reported. Herein, we prepare eutectic solvents based on urea as a hydrogen bond donor, [2-(methacryloyloxy)ethyl]trimethylammonium chloride (METAC) as a hydrogen bond acceptor, and 2-hydroxyethyl methacrylate (HEMA) as a comonomer to modulate physical properties, such as viscosity and hydrophilicity. METAC was used as the isolated salt, rather than as aqueous solution, to directly prepare water-free eutectic solvents with control over the final composition. These viscous, room-temperature stable liquids possess tunable glass transition temperatures and shear-dependent viscosity. Their direct photopolymerization, either *via* ultraviolet or visible-light-mediated methods and in the presence of crosslinker, gives rise to polyelectrolyte eutectogels with very high and tunable swelling capacity in aqueous media. The viscous nature of the eutectic mixture enables rapid photopolymerization kinetics compared to the equivalent process in water, with close to seven-fold increase in polymerization. Their cationic nature gives the gels inherent antimicrobial properties, as shown through their deactivation of *S. aureus* bacterial cells. Variation of the crosslinker concentration enables eutectic resins to be formed that show potential for direct ink writing (DIW) photopolymerization methods, highlighting the versatility of these materials.

1. Introduction

Polymeric eutectogels have emerged in recent years as a unique platform for the design of functional materials in areas such as wearable sensors,[1,2] topical approaches to drug delivery,[3,4] adhesives,[5,6] 3D printing[7,8] as well as electronics[9] and energy storage,[10–12] amongst numerous others. They are based on the inclusion of eutectic solvents within a three-dimensional (3D) polymer network, which may be either chemically or physically crosslinked to provide structural integrity. They are best viewed as structural analogues to hydrogels, which are 3D polymeric networks swollen with water. However polymeric hydrogels are susceptible to breakdown in materials properties (*e.g.* mechanical strength,[13,14] brittleness,[15] loss of or reduction in conductivity[16]) following the loss of absorbed water from the network *via* evaporation. Eutectic solvents (ESs) on the other hand typically have low volatility and high

thermal stability, enabling the material performance of eutectogels to be prolonged.

Research into eutectogels has progressed essentially in parallel with advances in ES and deep eutectic solvent (DES) design.[17,18] ESs are most typically prepared through the mixing of a hydrogen bond donor (HBD) (*e.g.* carboxylic acids, alcohols, amines, amides, amongst others) and a hydrogen bond acceptor (HBA) (often a quaternary ammonium salt, such as choline chloride)[19] to form a liquid with a melting point often significantly lower than either of the pure components. ESs represent an intriguing class of liquids with high solvation capacity, and tunable properties including viscosity, melting point, surface tension and conductivity.[20] Controversy remains with regards to their classification, given that all simple mixtures show a melting point depression regardless of whether ideal or non-ideal mixing has occurred.[18] Attempts have been made to quantify the "depth" of an ES,[21,22] which occurs due to favorable interactions between components, most typically *via* hydrogen bonding. More importantly, these solvents have unique properties and can be prepared by simply mixing relatively abundant, inexpensive, naturally occurring starting materials.[23–25] This obviates the need for discrete preparation *via* chemical synthesis, as is the case with ionic liquids, for example.

a School of Natural Sciences (Chemistry), University of Tasmania, Hobart, Tasmania 7005, Australia. E-mail: alexandra.mutch@utas.edu.au, stuart.thickett@utas.edu.au
b School of Chemical Engineering, University of New South Wales (UNSW), Sydney, NSW 2052, Australia. E-mail: edgar.wong@unsw.edu.au

†Electronic supplementary information (ESI) available. See DOI: https://doi.org/10.1039/d5lp00163c

In the context of preparing eutectogels, two main approaches are dominant. One is to prepare an "inert" ES (e.g. a mixture of choline chloride and urea), and to use this as a solvent for dissolution of monomers, crosslinkers, initiators and other additives. A variety of eutectogels have been prepared in this manner.[26–28] The second approach is what we term a "polymerizable eutectic" (PE), a subset of ESs whereby one or more component is a polymerizable species; the monomer now plays a dual role of reactant and solvent.[29] The large number of polar monomers amenable to chain polymerization has given rise to numerous examples of this approach, including PE-based eutectogels from acrylic acid,[30–32] acrylamide,[33] N-isopropylacrylamide,[34] itaconic acid,[15,31] 2-hydroxyethyl methacrylate,[35] amongst others. These have been used in the context of frontal polymerization,[36,37] UV and visible-light photopolymerization[30] (including 3D printing[38,39]), redox polymerization, in addition to controlled radical polymerization techniques.

Notably, the polymerizable eutectic approach is dominated by binary and ternary systems where the monomer plays the role of HBD, with a small molecule salt (such as a quaternary ammonium halide) used as an HBA. Reversing this approach, whereby the monomer is the HBA, is significantly less common, primarily due to the smaller number of commercial monomers that could act as an HBA. Examples include diallyldimethylammonium chloride (DADMAC), quaternary ammonium-based (meth)acrylamides, acrylates bearing betaine functionalities, and (meth)acrylate derivatives of choline chloride (ChCl), specifically [2-(methacryloyloxy)ethyl] trimethylammonium chloride (METAC). METAC is typically handled and subsequently polymerized as a concentrated aqueous solution, however its potential to act as an HBA in

PEs has been demonstrated by the groups of Mori,[40] Picchio and Mecerreyes.[41,42] Mori's group prepared a variety of PEs based on various quaternary ammonium monomers (isolated as salts) mixed with the classic HBD urea[40] to generate polyelectrolytes via solventless thermal free radical polymerization following multiple freeze–pump–thaw cycles; these polymers characterized with respect to their impressive ionic conductivity with a view towards energy storage applications. Mecerreyes and Picchio prepared a variety of quaternary ammonium PEs based on an aqueous solution of METAC and several HBDs including small-molecule phenols and polyphenols,[42] as well as citric acid;[41] following PE preparation the materials were freeze-dried to remove water, followed by polymerization. The resulting polymeric materials were shown to exhibit good CO_2 uptake, impressive adhesive properties, and inherent antimicrobial activity based on their quaternary ammonium structure within the polymeric repeat unit. This suite of properties makes quaternary ammonium PEs an exciting materials platform in numerous contexts.

In this work, we demonstrate the preparation, characterization and application of quaternary ammonium PEs for the creation of crosslinked eutectogels with tunable swelling capacity, rheological properties, in addition to good antimicrobial activity. These eutectogels were prepared using METAC as a polymerizable HBA, and urea as HBD, to generate viscous, room temperature stable liquids amenable to polymerization (Fig. 1). METAC was first isolated via precipitation and used as a salt, enabling the direct preparation of water-free eutectic solvents. A secondary monomer, 2-hydroxyethyl methacrylate (HEMA), was introduced as a functional additive to modulate both the rheological and thermal properties of the liquids, in addition to their swelling capacity
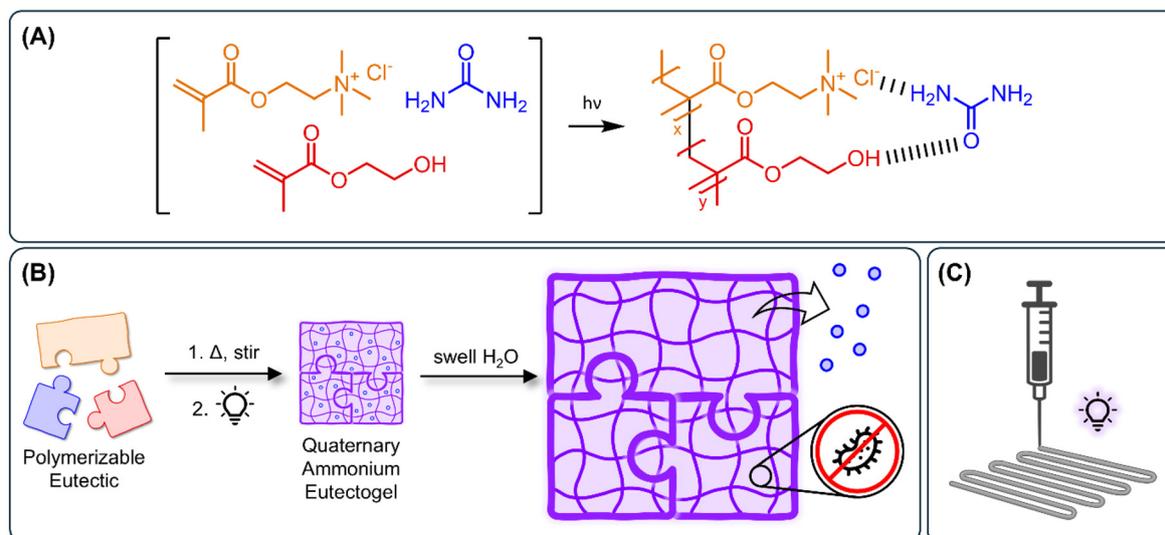
Fig. 1 (A) Scheme depicting the photopolymerization of METAC and HEMA from a polymerizable eutectic mixture with urea acting as HBD. (B) Overview of the preparation of quaternary ammonium eutectogels via photopolymerization of METAC and HEMA in the presence of a crosslinker, yielding networks with very high swelling ratios and antibacterial properties. During swelling urea is released from the eutectogel networks. (C) The polymerizable eutectic ternary mixture can be applied to direct ink writing 3D printing. This figure was prepared, in part, using BioRender.

once incorporated into eutectogels. It should be noted that HEMA can also participate in the hydrogen bonding network in the PEs, through its ester group and hydroxyl group, producing ternary eutectic mixtures. The eutectogels in this work were prepared *via* either UV photopolymerization or visible-light-mediated PET-RAFT polymerization with no deoxygenation, the latter PET-RAFT approach being the first such report of eutectogel preparation *via* this method. A significant rate enhancement was observed compared to the equivalent polymerization in water, attributed to the viscosity of the reaction medium. As quaternary ammonium polyelectrolytes, these gels exhibited good antimicrobial behavior towards model Gram-positive bacteria (*i.e.*, *Staphylococcus aureus*), which was further improved by the addition of "free" quaternary ammonium halide salts into the gel structure. Notably, the aqueous equivalent of these gels (*i.e.* polymerization of METAC and HEMA in water in the presence of crosslinker) lacked the structural integrity to retain its shape and structure when immersed in aqueous media – highlighting the novelty and benefit of using this eutectogel approach. As a final demonstration of the utility of this platform, these PEs were shown to enable simple direct ink writing (DIW) of various shapes through modulating the viscosity and crosslinker concentration, highlighting the future potential of these liquids in additive manufacturing.

2. Results and discussion

2.1. Characterization of polymerizable eutectic mixtures

We commenced our investigations by preparing mixtures of METAC and urea at various mole ratios, to identify compositions that would yield workable, room temperature liquids suitable for subsequent polymerization. Both METAC and urea are solids at room temperature; their capacity for hydrogen bonds to form between these compounds enables liquid mixtures to form upon heating and stirring. This PE was based on previous studies where a 1 : 2 METAC–urea ratio formed a viscous fluid,[40] and similar to the archetypal choline chloride–urea DES composition.[43] A room temperature liquid was formed at this composition (see Fig. S3†), albeit with exceedingly high viscosity (988 cP @ 298 K, 1 Hz, 0.1% strain). This "base mixture" was modified through the incorporation of

HEMA; the molar ratio of (METAC + HEMA)–urea was fixed at 1 : 2 whilst the internal mole fractions of METAC and HEMA were varied. For reference we refer to these METAC-HEMA–urea PEs using the abbreviation MHu-*x*, where *x* is the mole fraction of METAC in the monomer component. Room temperature liquids were formed for all compositions where *x* > 0.6 (see Fig. 2). The inclusion of HEMA into these PEs resulted in up to a ten-fold decrease in viscosity between the MHu-1.0 and the MHu-0.7 samples (see Fig. 4), whilst also influencing the hydrophilicity of the resulting eutectogels (see section 2.3).

Our MHu PEs were characterized by a combination of differential scanning calorimetry, FTIR, thermogravimetric analysis, as well as 1D/2D NMR spectroscopy. A series of representative ^{1}H NMR spectra related to the MHu-0.8 PE are shown in Fig. 3A–E. The spectrum of the PE following dissolution in the NMR solvent (Fig. 3D) displays all proton signals from the starting materials (urea, METAC and HEMA Fig. 3A–C, respectively), which supports that chemical transformations did not occur during the preparation of these PEs. The pure PEs were directly analyzed *via* NMR spectroscopy using a small glass capillary filled with deuterated solvent (Fig. 3E), with typical downfield shifts and line broadening observed. This is consistent with equivalent experiments examining other eutectic mixtures.[33,34,39,44,45] The line broadening is due to the high viscosity of these liquids, and peak shifting derives from the strong intermolecular interactions that exist between the components within the mixture. This was further supported *via* ^{1}H–^{1}H ROESY NMR spectroscopy, which revealed a series of correlations between the three PE components (see Fig. 3F). FTIR analysis indicated that peaks shifted as a result of eutectic formation, most notably those associated with the $-NH_2$ which is shown in Fig. S4 and S5.†

The solution diffusion behavior and viscoelastic properties of our PEs were evaluated using DOSY NMR spectroscopy and rheological analysis. DOSY NMR was used to evaluate the self-diffusion coefficients of the individual species in our PEs, as well as in comparison to the aqueous equivalents of these mixtures (*i.e.* METAC and HEMA dissolved in water where the mass fraction of water is the same as for urea in the ESs). The self-diffusion coefficients of these species are displayed in Fig. 4A, with tabulated data presented in Table S1.† We observe that for the MHu-1.0 PE (*i.e.* no HEMA), the self-diffusion coefficient of METAC ($\log_{10} D = -11.7 \pm 0.05$ m^2 s^{-1})


Fig. 2 Photo of MHu-*x* PE mixtures with molar ratios of *x*:(1 − *x*) : 2, where *x* represents the METAC fraction of the monomers as listed for each vial in the image.
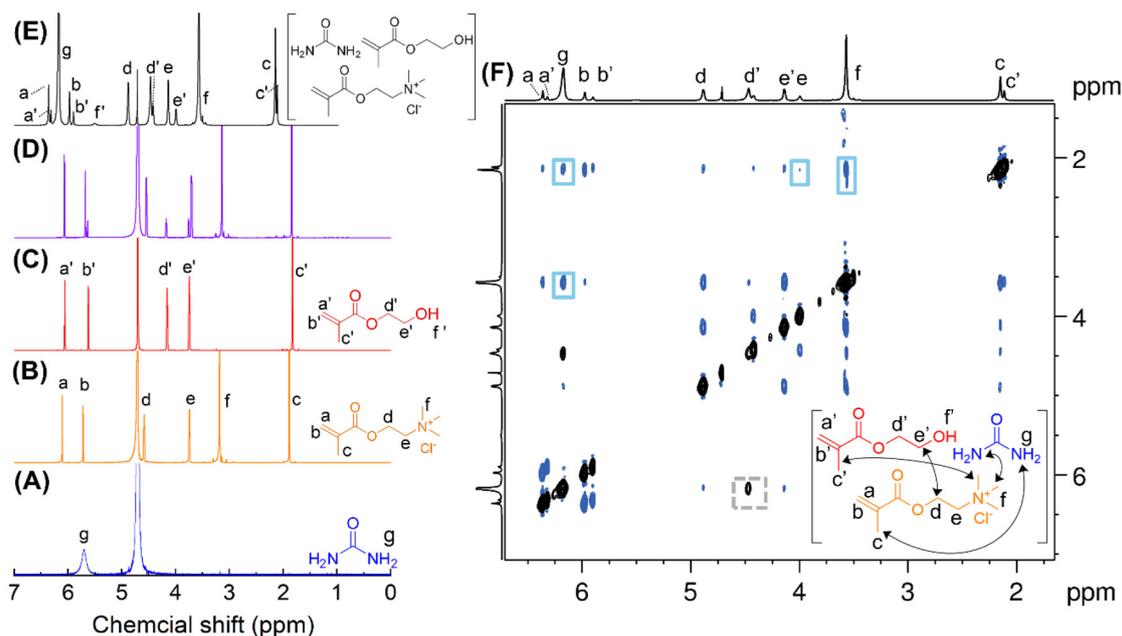
Fig. 3 ^{1}H NMR spectra of eutectic components (A) urea, (B) METAC, (C) HEMA, (D) the MHu-0.8 eutectic mixture dissolved in excess D$_2$O, and (E) the MHu-0.8 eutectic mixture with a sealed capillary containing D$_2$O. (F) ^{1}H$-^1$H ROESY NMR spectrum indicating major correlations within the MHu-0.8 eutectic mixture.
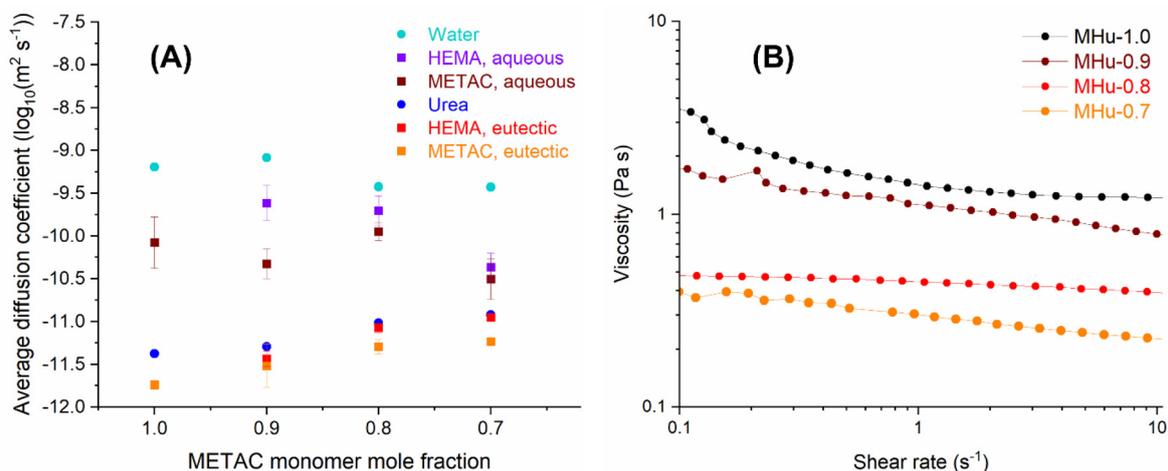

Fig. 4 (A) Self-diffusion coefficients of eutectic components obtained from DOSY NMR spectra of eutectic and aqueous mixtures at 50 °C. Data values are represented as the average of each proton peak ($n = 5$) in METAC and HEMA, respectively, standard error bars included. Proton signals of water and urea are also included for reference ($n = 1$). (B) Viscosity of eutectic mixtures as a function of shear rate at 50 °C.

is close to two orders of magnitude lower than when dissolved in water ($\log_{10} D = -10.1 \pm 0.30$ m^2 s^{-1}). As the mass fraction of HEMA increases, the self-diffusion coefficient of both METAC and HEMA increase. However, they remain significantly lower than their self-diffusion coefficient when dissolved in water. This result aligns with the viscosity of our PEs, which show a comparable trend. The Herschel–Bulkley model, a power-law relationship, was applied to the PEs where the consistency coefficient, K, of MHu-1.0 (1.44 ± 0.02 Pa s) was higher than MHu-0.7 (0.320 ± 0.001 Pa s), presented in Table S5.†

Consistency coefficient here refers to the viscosity at a shear rate of 1 Hz from a power law model fit, and where the power law index, n, is less than 1 for shear-thinning materials. Typical consistency coefficients for soft viscoelastic direct ink writing materials range from 10^{-1} to 10^3 Pa s.[46] Another important feature of the PEs is the effect of temperature (see Fig. S8†). The viscosity of the MHu-1.0 decreases from room temperature (25 °C, 9.8 Pa s) by more than a factor of ten at 50 °C (0.6 Pa s). For the PEs with HEMA present, the effect of temperature is less significant but still substantial; MHu-0.7 sees a 3-fold decrease
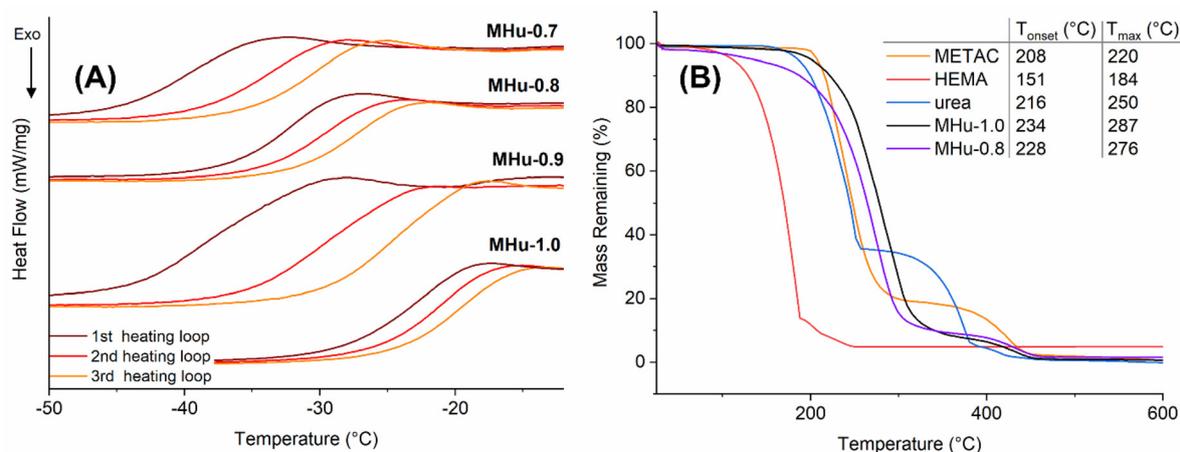
Fig. 5 (A) DSC thermograms of eutectic mixtures heated from −60 to 70 °C (first heating loop excluded). Thermograms from different samples have been offset for clarity. (B) TGA traces of eutectic components compared to the binary mixture, MHu-1.0 and the ternary mixture MHu-0.8, with onset and max rate temperatures tabulated.

across the temperature ramp studied. The high viscosity of the PEs has significant implications with regards to polymerization kinetics (see subsequent discussion).

Differential scanning calorimetry (DSC) analysis showed that for all compositions, these PEs were molecular glasses, with no distinct melting point observed over a wide temperature range; instead a glass transition that was a function of resin composition (see Fig. 5A). The measured T_g was tunable and was shown to decrease with increasing HEMA content, with all T_g values well below 0 °C and depressed as low as −39 °C (see Table S2†). Other examples of eutectic glasses have been previously reported,[47,48] however, this is relatively uncommon in comparison to those that possess a distinct melting point. We also observed a reproducible increase in the measured T_g upon multiple heating and cooling loops, with each loop resulting in an increase in T_g of the order of 1–2 °C. This phenomenon was observed over as many as 10 heating loops (see Fig. S6†). This is attributed to residual water in the PEs from their preparation, acting as a plasticizer, as reported by other groups.[24,49] To verify this, isothermal TGA analysis at 70 °C was performed on the MHu-0.7 sample, showing ~6.5–7% mass loss over 5 hours of heating (see Fig. S7†); this temperature was chosen as it was the maximum temperature of the DSC analysis used here. Upon continual heating under DSC conditions, water is lost from the eutectic, resulting in an increase in the measured T_g. TGA analysis of the PEs (see Fig. 5B) in comparison to their individual components showed an increase in the thermal stability; the onset decomposition temperature and maximum decomposition temperature increased by up to 18 °C and 37 °C, highlighting the thermal stability of these materials.

2.2. PE photopolymerization kinetics

Our PEs were then photopolymerized in a solvent-free manner, either using UV or visible (green) light irradiation, to prepare linear polymers for evaluation of polymerization kinetics. This was achieved by using a RAFT agent and either diphenyl(2,4,6-trimethylbenzoyl)phosphine oxide (TPO, as a Type I UV active photoinitiator) or Eosin Y (as a Type II visible light photoinitiator). Yu's group previously reported the blue and green-light mediated PET-RAFT polymerization of four vinyl monomers in an ethylene glycol/tetrabutylammonium chloride DES, however this work is the first such evaluation of polymerization kinetics in a PE.[50,51] These additional components were added to the PE with heating and stirring to ensure complete mixing and dissolution of solid reagents.

Photopolymerization kinetics of our PEs were monitored using FTIR spectroscopy (see Fig. 6 for data corresponding to the MHu-0.9 system) for both green light and UV irradiation and compared to the equivalent aqueous system (i.e. monomers dissolved directly in water at the same mass fraction as in our PEs). This was achieved by monitoring the change in peak height at 1320 cm^{-1}, which is associated with one of the vinyl protons throughout curing. A significant rate enhancement (>7 fold) in our PE is observed compared to water – using green light irradiation, the initial pseudo first-order rate coefficient for polymerization (over the time period 0–4 min) is 0.46 min^{-1} in our PE compared to 0.06 min^{-1} in water, with a fractional conversion of 80% achieved in ~4 min in the PE compared to ~9 min in water. Using UV light and an appropriate photoinitiator (TPO), the polymerization is even more rapid, with 80% fractional conversion achieved in approximately 30 s (see Fig. 6B). Quantification of reaction rates for the aqueous UV-initiated systems as a comparison was difficult due to a lack of homogeneous curing. To compare these systems, the final conversion of MHw-0.9 was determined by curing an aliquot of this sample directly in an NMR tube for 2 min. This MHw-0.9 conversion was only 28.3% after 2 min, compared with 95.7% for the MHu-0.9 sample over the same period. Such rate enhancements have been observed previously in the polymerization of other PEs; our group reported a
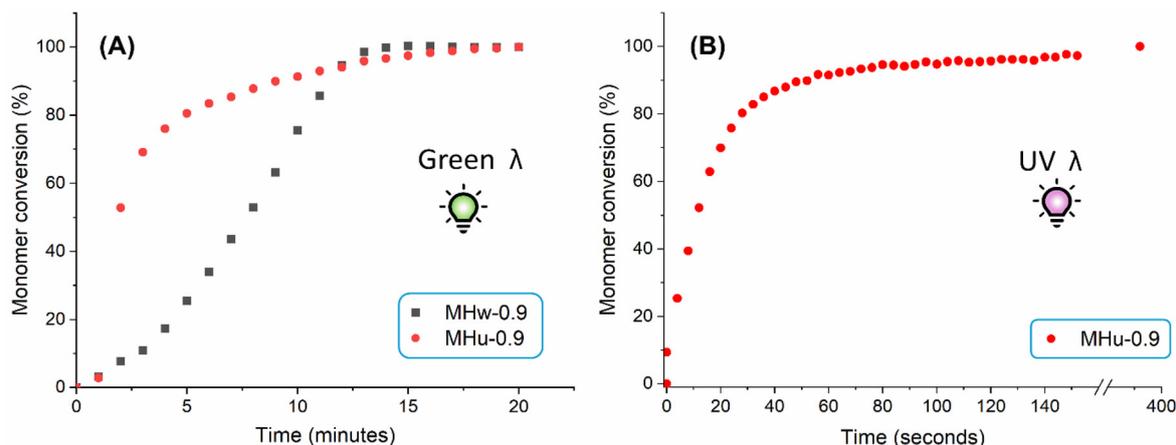
Fig. 6 (A) Kinetics of green light-initiated resins, comparing rates of aqueous equivalent, MHw-0.9 and PE, MHu-0.9. (B) Kinetics of UV-initiated MHu-0.9.

seven-fold rate increase in NIPAM-based PEs,[34] whilst Bednarz *et al.* saw a 20-fold rate increase in eutectogels based on itaconic acid.[52] This rate increase is attributed to the high viscosity of the reaction medium, reducing the effective rate of termination in free-radical polymerization. Other factors such as enhanced propagation kinetics due to hydrogen bonding of the reactive center cannot be excluded and would further increase the polymerization rate.[53,54]

2.3. Swelling properties of bulk photocured eutectogels

To prepare crosslinked eutectogels, poly(ethylene glycol) dimethacrylate (PEGDMA) was added to the PE mixture at a loading of 2 w/w% relative to monomer, the mixtures were then poured into molds and directly photopolymerized under UV irradiaton. As cationic polyelectrolyte eutectogels, our materials swelled significantly in water due to their highly hydrophilic nature (see Fig. 7A). The equilibrium swelling ratio S_{eq} of our eutectogels decreased upon increasing HEMA content, which is expected based on the more hydrophobic

nature of HEMA in comparison to METAC.[55] All eutectogels have very high swelling capacity ($S_{eq} \sim 40$–160) at room temperature, whilst retaining their original cured shape. The swollen gels become increasingly opaque as the HEMA content is increased. Swelling kinetics of our eutectogels in water (see Fig. 7B) were studied across 24 h. The Korsmeyer-Peppas mass transfer model,[56]

$$M_t/M_\infty = K \cdot t^n \tag{1}$$

was applied to study swelling kinetics across the first period of gel swelling (<20 min), where K represents the diffusion constant, and n represents the exponent pertaining to the mass transport behavior, for the first 15 min of swelling. All eutectogels had an exponent n in the range 0.63–0.68, suggesting "anomalous" or non-Fickian (case II) diffusion. This is characterized by a sharp front between the swollen and glassy parts of the gel as the solvent penetrates the material, which in our case we attribute to the initially high resin viscosity and crosslink density. Notably, the equivalent aqueous gels do not
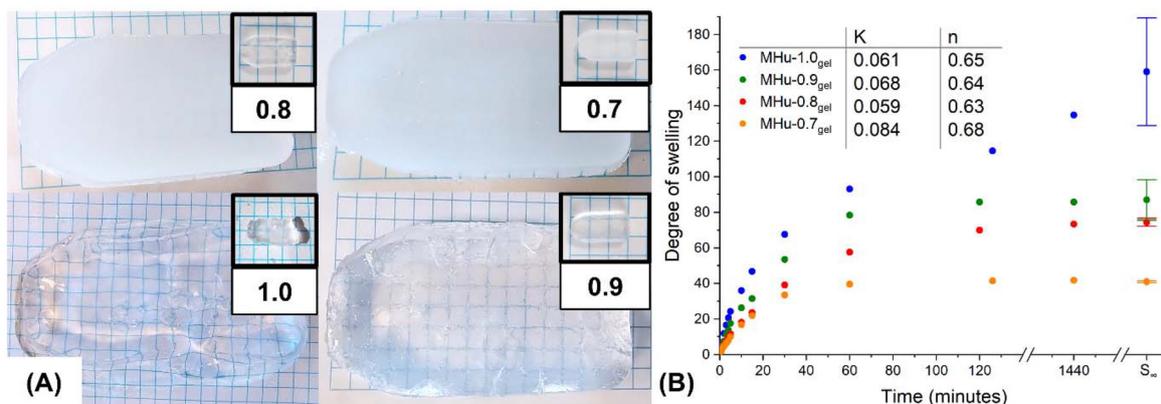
Fig. 7 (A) Photos of eutectogels at S_{eq} with their size as cured shown in insets. Light blue grid lines are 5 × 5 mm. (B) Swelling kinetics and swelling ratios. Error bars for eutectogels at equilibrium swelling represent standard deviation, n = 3. Inset text shows fit parameters for the Korsmeyer-Peppas mass transfer model for gel swelling.

© 2025 The Author(s). Published by the Royal Society of Chemistry

retain their structure when immersed in water, ultimately disintegrating. From a materials application context, this is important as our PE methodology yields eutectogels with sufficient structural integrity for subsequent applications, something not possible when preparing aqueous hydrogels from these monomers. Rotational rheometry showed that the eutectogels were stable across a temperature range of 20 to 55 °C (see Fig. S9†). The complex modulus (G^*) of the eutectogels increased with the addition of HEMA, ranging from 10^3 Pa for MHu-1.0$_{gel}$ to 10^4 Pa for the MHu-0.7$_{gel}$ sample.
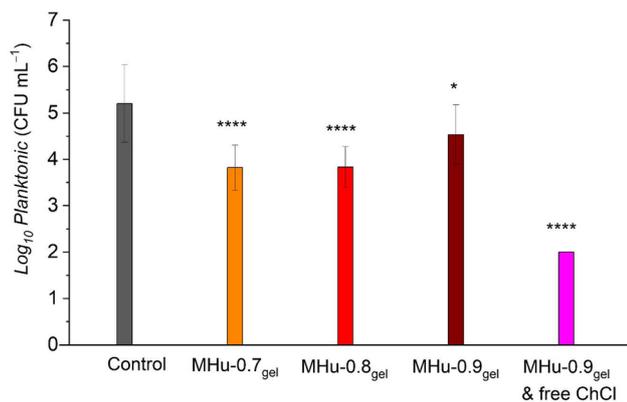
2.4. Antimicrobial performance of bulk-cured eutectogels

Given that METAC has been employed in the design of antimicrobial polymers because of its cationic nature,[57,58] we subsequently investigated the ability of the eutectogels to deactivate bacteria. Specifically, we tested the eutectogels against a model Gram-positive pathogen *Staphylococcus aureus* by soaking the swollen gel samples in the presence of bacteria solution at 37 °C for 24 h, followed by colony forming unit (CFU) analysis to determine the number of viable bacteria cells remaining in the solution after incubation (see Fig. 8). As observed in Fig. 8, MHu-0.9$_{gel}$, with the highest METAC content, resulted in poorer antimicrobial activity (0.7 $\log_{10}$ reduction in CFU per mL) compared to MHu-0.7$_{gel}$ and MHu-0.8$_{gel}$ (both showed 1.4 $\log_{10}$ reduction in CFU per mL) that possess lower METAC and higher HEMA content. As HEMA is more hydrophobic than METAC, the results here suggest that the incorporation of more hydrophobic HEMA units in place of METAC improve the antimicrobial performance of the eutectogels, possibly through increased perturbation of the bacteria cell membranes that eventually result in cell death, similar to previously reported work.[59,60] An additional eutectogel (based on MHu-0.9$_{gel}$) was fabricated where 10 mol% of METAC was replaced with free quaternary ammonium compound ChCl to determine if the antimicrobial activity could be improved upon. In addition to possessing antimicrobial activity, ChCl is also commonly used in the preparation of ESs and hence represents an excellent choice to replace METAC for this purpose. Indeed, the ChCl containing gel exhibited excellent antimicrobial efficacy, resulting in at least 3.2 $\log_{10}$ reduction in CFU mL^{-1} compared to the untreated control. Notably, no bacteria colonies were actually detected within the detection limit of 2 $\log_{10}$ in CFU mL^{-1}. The increased mobility of quaternary ammonium ions, either through leaching of ChCl into the solution or rearrangement within the gels upon contact with the bacteria, is postulated to have led to enhanced antimicrobial activity in this case.

2.5. Direct ink writing from PE-based resins

To further evidence the utility of these PEs, we demonstrated that by adjusting the crosslinker concentration, the PEs possess relevant rheological properties for their use as direct ink writing (DIW) resins for rapid photocuring into simple two-dimensional shapes. By increasing the PEGDMA concentration to 30% w/w, the MHu-0.7 PE forms a viscous yet free-flowing liquid that can be extruded from the nozzle of a polypropylene syringe (Fig. 9B); at the lower cross-linker concentrations used previously (2% w/w), the PE was too viscous and tacky to be successfully extruded. The DIW PE possessed a yield stress of 6.6 Pa at room temperature, moduli crossover at 1.83% shear strain ($G' = G'' = 87$ Pa), and a thixotropic recovery of 77% (see Table S6 and Fig. S12†) The PE, with the inclusion of PEGDMA and TPO as UV-active photoinitiator, was successfully extruded into simple shapes onto a glass slide, followed by 5 s of UV irradiation to rapidly photocure the resin into a free-standing eutectogel, and then a further 30 s irradiation after all layers were deposited to ensure structure was fully cured (Fig. 9D). These simple examples show the potential for these resins to be used in DIW printing, given their rapid photocuring and relevant rheological properties.

3. Experimental section

3.1. Materials

[2-(Methacryloyloxy)ethyl]trimethylammonium chloride (METAC) solution, 75 wt% in H$_2$O, urea (≥99%), 2-hydroxyethyl methacrylate (HEMA, 97%), poly(ethylene glycol) dimethacrylate (PEGDMA, average M_n 750), diphenyl(2,4,6-trimethylbenzoyl)phosphine oxide (TPO, 97%), Eosin Y (2′,4′,5′,7′-tetrabromofluorescein) disodium salt (EY), triethanolamine (TEOA, 99%), dimethylformamide (DMF, 99.8%), agar (microbiology tested) were purchased from Sigma-Aldrich. 2,2′-[Carbonothioylbis(thio)]bis[2-methylpropanoic acid] (CTBTBPA, 97%) was purchased from Boron Molecular. Deuterium oxide (D$_2$O) was purchased from Cambridge Isotope Laboratories. Mueller Hinton Broth (MHB, dehydrated), tryptone and yeast extract powder were purchased from Oxoid. Sodium chloride (laboratory grade) was purchased from Chem-supply. METAC was precipitated *via* acetone, dried
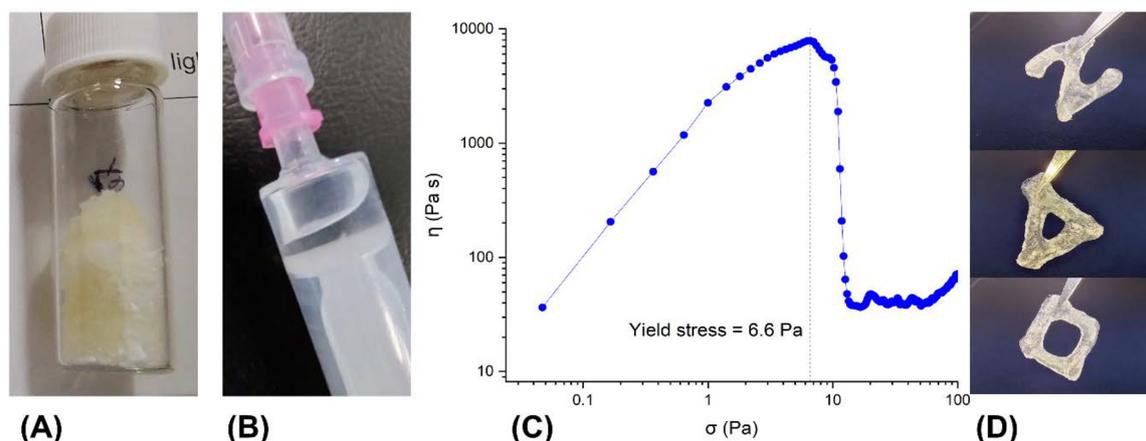

Fig. 8 Amount of planktonic *S. aureus* bacteria cells remaining, as determined by CFU analysis, after treatment with swollen gel samples for 24 h at 37 °C in PBS solution (pH 7.4). Two-tailed Student's *t*-test; asterisks indicate a statistically significant difference compared to the control sample [*$p < 0.1$; **$p < 0.01$; ***$p < 0.001$; ****$p < 0.0001$; NS, nonsignificant ($p > 0.1$)].

© 2025 The Author(s). Published by the Royal Society of Chemistry

RSC Appl. Polym., 2025, **3**, 1303–1314 | **1309**

Fig. 9 (A) Components for MHu-0.7 based resin to be used in DIW before heating and forming eutectic. (B) MHu-0.7 based resin loaded into syringe; material is transparent and viscous. (C) Yield stress of DIW resin. (D) Photos of structures (a letter Z, a triangle and a square) printed *via* manual DIW, *via* extrusion from a syringe followed by UV photocuring.

under vacuum for at least 24 h and stored in a desiccator. HEMA and PEGDMA were filtered through a short column of basic alumina to remove inhibitors; all other reagents were used as received.

3.2. Characterization

Nuclear magnetic resonance (NMR) spectroscopy was carried out on a Bruker Avance III HD 600 MHz spectrometer equipped with a 5 mm broadband tunable probe (BBFO) with a *z*-gradient. D_2O was used as a solvent for all ^1H spectra and polymerization kinetics experiments, and the temperature was maintained at 27 °C unless otherwise specified. For ROESY and DOSY experiments, D_2O was sealed in a glass capillary tube to prevent it dissolving the PEs. For the ROESY and DOSY experiments, the temperature was set to 50 °C.

The emission spectrum of the LED strips (λ_{max} = 521 nm) and the UV lamp (SUN 54 W UV LED lamp, λ_{max} = 370 nm) were measured using a USB2000+XR1-ES spectrometer with a fiber optic probe (Ocean Insight) and SpectraSuite data analysis software (see Fig. S1 and S2† for further details).

Thermogravimetric analysis (TGA) was performed with a NETZSCH Jupiter STA449 TGA-DSC instrument. Samples (5–10 mg) were placed in an alumina crucible (100 μL) and heated from 25 to 600 °C at a rate of 10 K min^{-1} in a high purity N_2 atmosphere.

Differential scanning calorimetry (DSC) was performed using a NETZSCH Caliris 300 DSC instrument and a refrigerated cooling system (RCS40). Samples (5–10 mg) were sealed in pierced *Concavus* aluminium pans and analyzed under a N_2 atmosphere (20.0 mL min^{-1}). Dynamic steps were conducted at 10 K min^{-1} unless otherwise specified. For the experiments cooled to −60 °C and heated to 70 °C, isothermal holds after the cooling loops were held for 15 min and 10 min after a heating loops. For experiments cooled to −70 °C and heated to 0 °C, isothermal holds after the cooling loop were held for

20 min to allow for enough time for temperature to equilibrate. Data presented is from the second run onwards to investigate phase transition behavior.

FTIR spectra were acquired on a PerkinElmer Spectrum 100 Fourier-transform infrared spectrometer using a single reflection diamond/ZnSe ATR in the range of 4000–600 cm^{-1} with a spectral resolution of 4 cm^{-1}. 32 scans were used for the background and sample measurement. Green light kinetics were conducted on the PerkinElmer FTIR by placing a droplet of the resin directly on the ATR crystal and then irradiating. A Shimadzu IRXross FTIR spectrometer was used to measure the UV light curing kinetics.

Rheological analysis was carried out using a NETZSCH Kinexus pro + rheometer with a parallel plate-plate configuration. Stainless steel plates were used with an upper plate diameter of 20 mm. Experiments on eutectic compositions of METAC-HEMA–urea were performed at 50 °C, and at 25 °C for the eutectogel and ink study, unless otherwise stated. For the eutectic compositions and the ink, a working gap of 0.5 mm was used. An amplitude sweep was carried out from shear strains of 0.1 to 100% at a frequency of 1 Hz to determine the linear viscoelastic region. Shear rate sweeps were carried out from 0.1 to 10 Hz at a shear strain of 0.5%. Temperature ramp experiments were conducted from 25 to 50 °C at a ramp rate of 1 °C at a frequency of 1 Hz and a shear strain of 0.1% and sampling interval of 2 s. Stress ramps were conducted from 0 to 200 Pa over a time interval of 2 min to investigate the yield stress of samples, with a trigger set to stop once the sample shear rate is greater than 5 Hz. The material used for the DIW was analyzed with an amplitude sweep (0.01 to 100%), stress ramp (shear stress rate >5 Hz), shear rate sweep (0.01 to 100 Hz in 120 s), and a three-step shear test to determine thixotropic behavior (120 s at 0.1 Hz; 120 s at 100 Hz; 600 s at 0.1 Hz). For the fully hydrated eutectogels, amplitude sweeps (0.01 to 100%) and temperature ramps (20 to 55 °C at 1 Hz, 1%) were performed.

3.3. Preparation of polymerizable eutectics

An example eutectic procedure is detailed as follows. A eutectic composed of METAC–HEMA–urea with a molar ratio of 0.9 : 0.1 : 2 (MHu-0.9) was prepared in a 4 mL capped glass vial. The three reagents were added to the vial with a magnetic stirbar (300 rpm) and heated to 90 °C for 1 h, until the mixture became transparent and viscous. This was performed for 11 eutectic compositions, varying the ratio of METAC and HEMA. Aqueous equivalents of these samples were prepared in the same manner, replacing urea with water, in the same mass ratio, and given the code MHw-x. For subsequent experiments, mixtures were prepared using MHu-x, where x > 0.6, as these resulted in homogeneous stable PEs.

Photopolymerization reactions were carried out under visible light irradiation in a custom-built photoreactor (see Fig. S1†). The kinetics of linear polymerization were monitored as follows: resins were prepared using MHu PEs and a photoinitiator (either TPO or EY and TEOA, with ratios as per the following section) and placed on the ATR-FTIR detector. Spectra were recorded at regular intervals (every minute for curing under green light, and every 5 s for curing under UV light). The transmission of the peak at 1320 cm^{-1} associated with one of the vinyl monomers was recorded at regular intervals, and the relative curing was calculated by the following equation:

$$\mathrm{Conversion}(\%) = \frac{T_i - T_t}{T_i - T_f} \qquad (2)$$

where T_i is the transmission value before being cured, T_t is the transmission value at any respective time point, and T_f is the transmission value of the fully cured sample.

For polymerizations performed over longer timescales (>1 h), the kinetics were monitored via ^{1}H NMR via the consumption of the vinyl proton at chemical shift 6.1 ppm relative to DMF at 7.9 ppm (see Fig. S10 and S11† for a representative spectra).

3.4. Preparation of bulk photocured polymeric materials from polymerizable eutectics

Note that w/w % are given with respect to total monomer mass. The crosslinker (2 w/w% PEGDMA), CTBTBPA (target 400 DP), photoinitiator (0.2% w/w TPO, 7 μg mg^{-1} in DMF), were added together with the eutectic components. All the reagents were heated together at 90 °C for 1 h until the mixture became transparent and viscous. The resin was poured into a flat embedding mold (PTFE), and a heat gun was used to level the resin out. The molds were irradiated with a UV lamp for 2 min, the sample was removed from the mold and flipped, and further irradiated for another 2 min.

This same method was used to prepare resins for PET-RAFT polymerizations by replacing TPO in DMF with EY in DMF (0.2% w/w, 7 μg mg^{-1} in DMF) and TEOA (2000 : 1 molar ratio with respect to EY) with irradiation under green light for 15 min.

3.5. Swelling investigation of bulk photocured polymer materials from polymerizable eutectics

The cured gels were weighed after curing (m_d) and then placed in excess distilled water (20 °C). The gels were periodically removed from the water using a strainer, gently dried with a lint-free tissue, and its mass was recorded. The swelling ratio, S, of the gels was calculated as:

$$S = \frac{m_s - m_d}{m_d} \qquad (3)$$

where m_s is the mass of the fully hydrated gel, and m_d is the mass of the dry gel.

3.6. Antimicrobial testing

The bactericidal efficiency of the eutectogels was evaluated against Gram-positive pathogen *S. aureus* ATCC 29213. Briefly, a single bacterial colony was cultured in 10 mL of Mueller–Hinton Broth (MHB) at 37 °C with 180 rpm shaking overnight. Meanwhile, the gel samples were fully soaked in phosphate-buffered saline (PBS, pH 7.4) for 24 h, then weighed (*ca.* 10 mg) and transferred to a 24-well microplate (Costar, Corning). The overnight bacteria culture was diluted to *ca.* 10^6 colony forming units (CFU) per mL in PBS (*ca.* 100-fold dilution) for the killing study. The diluted bacteria suspension (*ca.* 1 mL per 10 mg of swollen eutectogel) was then added into the wells containing the pre-swelled eutectogels. A negative control, that is simply a 1 mL bacterial suspension without eutectogels, was also included in the assay. The microplate was incubated for 24 h at 37 °C, followed by ultrasonication (150 W, 40 kHz, Australia) for 10 min to detach cells that may have attached to the surface of the eutectogels. The viability of planktonic cells in the solution of each well was then determined by a drop plate method where the planktonic cells were serially diluted in PBS and plated onto Luria Bertani agar. After 24 h of incubation at 37 °C, bacteria colonies were counted and CFU analysis was performed. The assay included two replicates and were repeated in two independent experiments.

3.7. Manual direct ink writing

In order to perform direct ink writing tests, the MHu-0.7 eutectic mixture, CTBTBPA (target 400 DP), PEGDMA (30 w/w%), and TPO (1 w/w%) was prepared with heating and stirring as mentioned above and then in a dark room, poured into a polypropylene 5 mL syringe (Norm-Ject®, Luer-Slip), with the polyethylene plunger removed, which was covered in aluminium foil to minimize polymerization in the syringe. A blunt needle (18 G × 38 mm) was then attached and when the ink had cooled to room temperature, the excess headspace in the syringe was expelled. At this point the ink could be deposited into the desired shape. A glass slide was used for good adhesion. A pattern was manually drawn on the slide, exposed for 5 s to UV light and then the pattern was repeated on the previous layer for a total of three or four layers. The final shape

was then exposed to UV light for 30 s to ensure complete curing.

4. Conclusions

In conclusion, we showcased the development of quaternary ammonium eutectogels through the rational design of a polymerizable eutectic based on a quaternary ammonium methacrylate salt, urea, and a co-monomer (2-hydroxyethyl methacrylate) to regulate the thermal and rheological properties of both the starting resin and resulting eutectogel. The eutectogels were shown to exhibit rapid photopolymerization kinetics, both under green and UV LED irradiation, enabling solvent-free polymerization in minutes using relatively benign reaction conditions, with no deoxygenation. The high polymerization rate is attributed to the high viscosity of these systems and hence low self-diffusion coefficient of the reacting species, promoting faster kinetics in comparison to the equivalent aqueous polymerization. The eutectogels are extremely hydrophilic, showing significant and tunable swelling capacity and rheological properties in water. Their cationic nature enables them to be inherently antimicrobial, as shown by the reduction in *S. aureus* population when exposed to these gels. The antimicrobial capacity of these materials was further enhanced with the inclusion of free quaternary ammonium salts within the gel matrix. Furthermore, rheological modulation through varying the crosslinker concentration enables these materials to be suitable candidates for DIW printing, *via* extrusion and subsequent curing. We anticipate that the tuneability of the material properties of this polymerizable eutectic platform will open numerous future opportunities in the design of antimicrobial materials that can be printed or cast into tailored shapes.

Author contributions

A. N. – data curation, formal analysis, investigation, methodology, project administration, visualization, writing – original draft, writing – review and editing. Z. S. – data curation, formal analysis, investigation. A. C. B. – conceptualization, supervision, writing – original draft, writing – review and editing. E. H. H. W. – methodology, project administration, resources, visualization, supervision, writing – original draft, writing – review and editing. A. L. M. – formal analysis, project administration, supervision, visualization, writing – original draft, writing – review and editing. S. C. T. – conceptualization, funding acquisition, methodology, project administration, supervision, writing – original draft, writing – review and editing.

Conflicts of interest

There are no conflicts to declare.

Data availability

Data for this article, which includes: Visible-light LED photocuring equipment and spectral output; NMR and FTIR spectral data on binary and ternary eutectic mixtures; tabulated and graphical data from DSC traces; tabulated and graphical data from TGA thermograms; processed data from rotational and oscillatory rheometry can be found in the Electronic ESI† that accompanies the manuscript, and will also be provided upon request to the authors.

Acknowledgements

References

1 R. Svigelj, N. Dossi, C. Grazioli and R. Toniolo, *Sensors*, 2021, **21**, 4263.

2 P. A. Mercadal, A. González, A. Beloqui, L. C. Tomé, D. Mecerreyes, M. Calderón and M. L. Picchio, *JACS Au*, 2024, **4**, 3744–3758.

3 M. M. Abdelquader, S. Li, G. P. Andrews and D. S. Jones, *Eur. J. Pharm. Biopharm.*, 2023, **186**, 85–104.

4 S. Emami and A. Shayanfar, *Pharm. Dev. Technol.*, 2020, **25**, 779–796.

5 Y. Wan, S. Huang, Y. Sun, H. Zhu, Q. Zheng, Q. Zhang and S. Zhu, *Chem. Eng. J.*, 2022, **442**, 136289.

6 S. H. Jung, G. Choi, S. Jeong, J. Park, H. Yoon, J.-J. Park and H. Kim, *ACS Sustainable Chem. Eng.*, 2022, **10**, 13816–13824.

7 Y. Li, R. K. Kankala, L. Wu, A.-Z. Chen and S.-B. Wang, *ACS Appl. Polym. Mater.*, 2023, **5**, 991–1001.

8 C.-W. Lai and S.-S. Yu, *ACS Appl. Mater. Interfaces*, 2020, **12**, 34235–34244.

9 M. L. Picchio, A. Dominguez-Alfaro, R. J. Minari, J. D. Mota-Morales and D. Mecerreyes, *J. Mater. Chem. C*, 2024, **12**, 11265–11284.

10 O. E. Geiculescu, D. D. DesMarteau, S. E. Creager, O. Haik, D. Hirshberg, Y. Shilina, E. Zinigrad, M. D. Levi, D. Aurbach and I. C. Halalay, *J. Power Sources*, 2016, **307**, 519–525.

11 A. Sharma, R. Sharma, R. C. Thakur and L. Singh, *J. Energy Chem.*, 2023, **82**, 592–626.

12 D. Julião, M. Xavier and X. Mascarenhas, *Mater. Today Energy*, 2024, **42**, 101432.

13 X. Pan, J. Yu, X. Lu, Q. Wang, X. Ma, S. Cao and Y. Ni, *J. Colloid Interface Sci.*, 2022, **623**, 1151–1159.

14 T.-Y. Chen, Y.-J. Jiang and H.-W. Chien, *Polymers*, 2023, **15**(12), 2605.

15 S. Bednarz, M. Fluder, M. Galica, D. Bogdal and I. Maciejaszek, *J. Appl. Polym. Sci.*, 2014, **131**(16), 40608.

16 Y. Zhong, N. Lopez-Larrea, M. Alvarez-Tirado, N. Casado, A. Koklu, A. Marks, M. Moser, I. McCulloch, D. Mecerreyes and S. Inal, *Chem. Mater.*, 2024, **36**, 1841–1854.

17 M. Francisco, A. van den Bruinhorst and M. C. Kroon, *Angew. Chem., Int. Ed.*, 2013, **52**, 3074–3085.

18 D. O. Abranches and J. A. P. Coutinho, *Annu. Rev. Chem. Biomol. Eng.*, 2023, **14**, 141–163.

19 E. L. Smith, A. P. Abbott and K. S. Ryder, *Chem. Rev.*, 2014, **114**, 11060–11082.

20 A. T. H. Yeow, A. Hayyan, M. Hayyan, M. Usman Mohd Junaidi, J. Saleh, W. Jefrey Basirun, M. Roslan Mohd Nor, W. Al Abdulmonem, M. Zulhaziman, M. Salleh, F. Mohamed Zuki and M. Diana Hamid, *Results Chem.*, 2024, **7**, 101378.

21 A. Shishov, P. Makoś-Chełstowska, A. Bulatov and V. Andruch, *J. Phys. Chem. B*, 2022, **126**, 3889–3896.

22 V. Agieienko and R. Buchner, *Phys. Chem. Chem. Phys.*, 2022, **24**, 5265–5268.

23 Y. Liu, J. B. Friesen, J. B. McAlpine, D. C. Lankin, S.-N. Chen and G. F. Pauli, *J. Nat. Prod.*, 2018, **81**, 679–690.

24 R. Craveiro, I. Aroso, V. Flammia, T. Carvalho, M. T. Viciosa, M. Dionísio, S. Barreiros, R. L. Reis, A. R. C. Duarte and A. Paiva, *J. Mol. Liq.*, 2016, **215**, 534–540.

25 A. V. Gómez, A. Biswas, C. C. Tadini, R. F. Furtado, C. R. Alves and H. N. Cheng, *J. Braz. Chem. Soc.*, 2019, **30**, 717–726.

26 C. Mukesh, K. K. Upadhyay, R. V. Devkar, N. A. Chudasama, G. G. Raol and K. Prasad, *Macromol. Chem. Phys.*, 2016, **217**, 1899–1906.

27 B. Guo, M. Yao, S. Chen, Q. Yu, L. Liang, C. Yu, M. Liu, H. Hao, H. Zhang, F. Yao and J. Li, *Adv. Funct. Mater.*, 2024, **34**, 2315656.

28 J.-Y. Yang, A. Kumar, M. O. Shaikh, S.-H. Huang, Y.-N. Chou, C.-C. Yang, C.-K. Hsu, L.-C. Kuo and C.-H. Chuang, *ACS Appl. Mater. Interfaces*, 2023, **15**, 55244–55257.

29 Y. Nahar and S. C. Thickett, *Polymers*, 2021, **13**(3), 447–470, DOI: **10.3390/polym13030447**.

30 R. Li, G. Chen, M. He, J. Tian and B. Su, *J. Mater. Chem. C*, 2017, **5**, 8475–8481.

31 Y. Jin, J. Li, M. Zhang, J. He and P. Ni, *Chem. Commun.*, 2023, **59**, 12998–13001.

32 Y. Zhang, C. Liu, S. Zhang, J. Li, P. Quan, Y. Song, J. Liu and L. Fang, *Chem. Eng. J.*, 2023, **476**, 146583.

33 Y. Nahar, P. Wei, C. Cipriani, A. Khodabandeh, A. C. Bissember, E. B. Pentzer and S. C. Thickett, *ACS Appl. Polym. Mater.*, 2022, **4**, 8429–8440.

34 Y. Nahar, J. Horne, V. Truong, A. C. Bissember and S. C. Thickett, *Polym. Chem.*, 2021, **12**, 254–264.

35 H. Liu, X. Zhou, A. Nail, H. Yu, Z. Yu, Y. Sun, K. Wang, N. Bao, D. Meng, L. Zhu and H. Li, *J. Controlled Release*, 2024, **368**, 115–130.

36 J. D. Mota-Morales, M. C. Gutiérrez, M. L. Ferrer, I. C. Sanchez, E. A. Elizalde-Peña, J. A. Pojman, F. D. Monte and G. Luna-Bárcenas, *J. Polym. Sci., Part A:Polym. Chem.*, 2013, **51**, 1767–1773.

37 J. D. Mota-Morales, M. C. Gutiérrez, I. C. Sanchez, G. Luna-Bárcenas and F. del Monte, *Chem. Commun.*, 2011, **47**, 5328–5330.

38 N. Corrigan, A. L. Mutch, C. Boyer and S. C. Thickett, *RSC Appl. Polym.*, 2024, **2**, 914–925.

39 A. L. Mutch, Y. Nahar, A. C. Bissember, N. Corrigan, C. Boyer, X. Y. Oh, V. X. Truong and S. C. Thickett, *Macromol. Rapid Commun.*, 2024, **45**, 2400268.

40 K. Ajino, A. Torii, H. Ogawa and H. Mori, *Polymer*, 2020, **204**, 122803.

41 M. Isik, S. Zulfiqar, F. Edhaim, F. Ruiperez, A. Rothenberger and D. Mecerreyes, *ACS Sustainable Chem. Eng.*, 2016, **4**, 7200–7208.

42 J. L. De Lacalle, A. Gallastegui, J. L. Olmedo-Martínez, M. Moya, N. Lopez-Larrea, M. L. Picchio and D. Mecerreyes, *ACS Macro Lett.*, 2023, **12**, 125–132.

43 A. P. Abbott, G. Capper, D. L. Davies, R. K. Rasheed and V. Tambyrajah, *Chem. Commun.*, 2003, 70–71.

44 Y. Nahar, M. K. Stanfield, A. C. Bissember and S. C. Thickett, *Polym. Chem.*, 2023, **14**(22), 2724–2733.

45 A. L. Mutch and S. C. Thickett, *Polym. Chem.*, 2025, **16**, 1332–1344.

46 R. D. Weeks, J. M. Ruddock, J. D. Berrigan, J. A. Lewis and J. O. Hardin, *Adv. Intell. Syst.*, 2025, **7**, 2400293.

47 A. Alhadid, L. Mokrushina and M. Minceva, *J. Mol. Liq.*, 2020, **314**, 113667.

48 R. Craveiro, I. Aroso, V. Flammia, T. Carvalho, M. T. Viciosa, M. Dionísio, S. Barreiros, R. L. Reis, A. R. C. Duarte and A. Paiva, *J. Mol. Liq.*, 2016, **215**, 534–540.

49 T. Carvalho, V. Augusto, A. R. Brás, N. M. T. Lourenço, C. A. M. Afonso, S. Barreiros, N. T. Correia, P. Vidinha, E. J. Cabrita, C. J. Dias, M. Dionísio and B. Roling, *J. Phys. Chem. B*, 2012, **116**, 2664–2676.

50 Y.-T. Chou, W.-R. Lee and S.-S. Yu, *Macromolecules*, 2024, **57**, 9241–9249.

51 C.-Y. Li and S.-S. Yu, *Macromolecules*, 2021, **54**, 9825–9836.

52 S. Bednarz, K. Półćwiartek, J. Wityk, B. Strachota, J. Kredatusová, H. Beneš, A. Wesołowska-Piętak and G. Kowalski, *Eur. Polym. J.*, 2017, **95**, 241–254.

53 G. Schmidt-Naake, I. Woecht, A. Schmalfuß and T. Glück, *Macromol. Symp.*, 2009, **275–276**, 204–218.

54 B. De Sterck, R. Vaneerdeweg, F. Du Prez, M. Waroquier and V. Van Speybroeck, *Macromolecules*, 2010, **43**, 827–836.

55 I. Cárdaba, L. Porcarelli, A. Gallastegui, D. Mecerreyes and M. I. Maguregui, *Polymers*, 2021, **13**, 2108.

56 N. Corrigan, A. L. Mutch, C. Boyer and S. C. Thickett, *RSC Appl. Polym.*, 2024, **2**, 914–925.

57 T. Shiga, H. Mori, K. Uemura, R. Moriuchi, H. Dohra, A. Yamawaki-Ogata, Y. Narita, A. Saito and Y. Kotsuchibashi, *Polymers*, 2018, **10**, 947.

58 Y. Fu, Y. Yang, S. Xiao, L. Zhang, L. Huang, F. Chen, P. Fan, M. Zhong, J. Tan and J. Yang, *Prog. Org. Coat.*, 2019, **130**, 75–82.

59 J. Tan, Y. Zhao, J. L. Hedrick and Y. Y. Yang, *Adv. Healthcare Mater.*, 2022, **11**, 2100482.

60 T.-K. Nguyen, S. J. Lam, K. K. K. Ho, N. Kumar, G. G. Qiao, S. Egan, C. Boyer and E. H. H. Wong, *ACS Infect. Dis.*, 2017, **3**, 237–248.